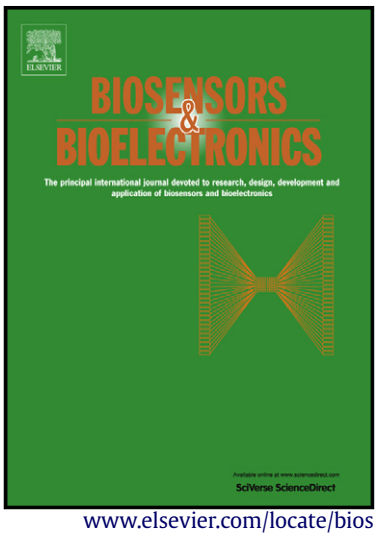

www.elsevier.com/locate/bios

A novel graphene-DNA biosensor for selective detection of mercury ions

Yang Zhang, Hong Zhao, Zhijiao Wu, Ying Xue, Xiaofang Zhang, Yujian He, Xiangjun Li, Zhuobin Yuan

PII: S0956-5663(13)00279-0
DOI: http://dx.doi.org/10.1016/j.bios.2013.04.013
Reference: BIOS5893

To appear in: *Biosensors and Bioelectronics*

Received date: 12 October 2012
Accepted date: 12 April 2013

Cite this article as: Yang Zhang, Hong Zhao, Zhijiao Wu, Ying Xue, Xiaofang Zhang, Yujian He, Xiangjun Li, Zhuobin Yuan, A novel graphene-DNA biosensor for selective detection of mercury ions, *Biosensors and Bioelectronics,* http://dx.doi.org/10.1016/j.bios.2013.04.013

A novel graphene-DNA biosensor for selective detection of mercury ions

Yang Zhang, Hong Zhao*, Zhijiao Wu, Ying Xue, Xiaofang Zhang, Yujian He, Xiangjun Li, Zhuobin Yuan

College of Chemistry and Chemical Engineering, University of Chinese Academy of Sciences, 19A YuQuan Road, 100049, Beijing, China

ABSTRACT

A novel electrochemical biosensor for sensitive and selective detection of mercury (II) ions (Hg^{2+}) based on a DNA grafted graphene is proposed. Graphene oxide (GO) was reduced by dopamine, and then the single-strand probe DNA modified at the 5'-end with an alkylamino modifier (NH_2-ssDNA) was grafted on the reduced graphene oxide (RGO) surface via Michael addition reaction. In the presence of Hg^{2+}, the target DNA with four thymine-thymine (T-T) mismatches would hybridize with the probe DNA on the glassy carbon electrode (GCE) through T-Hg^{2+}-T coordination chemistry. The hybridization of the two oligonucleotides leads to the increase in the peak currents of $[Ru(NH_3)_6]^{3+}$, which could be used for electrochemical sensing of Hg^{2+}. The difference in the value of the peak currents of $[Ru(NH_3)_6]^{3+}$ before and after DNA hybridization was linear with the concentration of Hg^{2+} in the range from

* Corresponding author. Tel: +86-10-88256827; Fax: +86-10-88256092.
E-mail addresses: hongzhao@gucas.ac.cn

8.0×10^{-9} to 1.0×10^{-7}M with a linear coefficiency of 0.996. The detection limit was 5.0×10^{-9} M (S/N=3). The proposed electrochemical biosensor is rapid, convenient and low-cost for effective sensing of Hg^{2+}. Particularly, the proposed method was applied successfully to the determination of Hg^{2+} detection in real environmental samples.

Keywords: mercury ions, graphene, Michael addition, biosensor, nucleic acids

1. Introduction

Mercury is a potent neurotoxin as it can accumulate in the vital organs and tissues binding with sulfur-containing proteins and enzymes, some important cell functions are inactivated which result in a wide variety of diseases (Harris et al., 2003). Particularly, mercury harmfully affects the function and development of the central nervous system in people. Therefore, exposure to mercury is potentially dangerous for human beings, especially for children. However, mercury pollution is a serious environmental health problem all over the world. Thus, growing attentions have been paid for the determination of mercury ions. Traditional analytical techniques including atomic absorption spectroscopy (AAS), atomic fluorescence spectrometry (AFS), inductively coupled plasma mass spectrometry (ICP-MS) (Butler et al., 2007), and X-ray absorption spectroscopy (Bernaus et al., 2006) have been widely used for measuring Hg^{2+}. These methods are time-consuming and require complicated instruments. Recently, several methods have been proposed for the detection of mercury ions such as fluorescent probes (Wu et al., 2007; Lee et al., 2009),

conjugated polymers (Fang et al., 2008), polymeric materials (Zhao et al., 2006), proteins (Gu et al., 2011), oligonucleotides (Joseph et al., 2011), gold nanoparticles (Hung et al., 2010), carbon nanotube (McNicholas et al., 2011) and nanophosphors (Liu et al., 2011). However, most of these methods have some limitations such as poor selectivity with interference of other metals, insufficient sensitivity and cost-consuming instruments. In 2006, the Akira Ono group reported that T-T mismatches could selectively capture Hg^{2+} to form T-Hg^{2+}-T base pairs (Miyake et al., 2006), as the intrinsic specific interaction between Hg^{2+} and thymine, this strategy could provide a high selectivity toward Hg^{2+} over other related environmental heavy metal ions. Then a series of Hg^{2+} biosensors based on T-Hg^{2+}-T are developed afterwards (Wu et al., 2010). The Mirkin group use gold nanoparticles combined with DNA to detect Hg^{2+}, the limit of detection is 10 nM (Lee et al., 2008). The Liu group synthesized hydrogel microparticles with covalently attached DNA probes, detect Hg^{2+} with a fluorescence change, the limit of detection is 10 nM (Dave et al., 2010; Helwa et al., 2012). And some other T-Hg^{2+}-T biosensors for Hg^{2+} detection (Wen et al., 2011; Liu et al., 2010) are also reported. Fox example, Mo et al. researched the influences of strand length and the number of thymine base (T) for Hg^{2+} detection by quartz crystal microbalance (QCM) (Mo et al., 2009). As the limit amount of mercury ions in drinking water recommended by the World Health Organization (WHO) and Environmental Protection Agency (EPA) are respectively 5 nM and 10 nM (Aragay et al., 2012), sensitive methods are still urgent for analyzing mercury ions.

Graphene, a new two-dimensional(2D) structure which consists of sp^2-hybridized

carbon, has attracted extensive attentions in recent years for its outstanding features, such as high electrical conductivity, large surface area, rapid heterogeneous electron transfer, high mechanical strength and good biocompatibility (Novoselov et al., 2005; Meyer et al., 2007; Geim et al., 2007; Zhang et al., 2005; Pumera, 2010; Zhao et al., 2010; Wang et al., 2011). Thus graphene has great potential applications in many areas, including nanoelectronics, supercapacitors, batteries and sensors. Especially, graphene-DNA biosensors could establish a biorecognition platform with extraordinary sensitivity, rapid readout, and good biostability (Lu et al., 2009; Tang et al., 2010a; Stine et al., 2010; Tang et al., 2010b), thus graphene-DNA biosensor has become a hot spot of research. Recent studies have shown that most of graphene-DNA biosensors were built via adsorption effect between the nucleotides and graphene surface (Wu et al., 2011; Zhang et al., 2011a; Bonanni et al., 2011; Tang et al., 2011) or the condensation reaction between the amino group of amino-modified DNA and carboxylic group of graphene oxide (GO) (Feng et al., 2011; Bonanni et al. 2012; Dubuisson et al., 2011). The adsorption method was simple and quick, but it might be instable and thus leading to a worse reproduction. The condensation reaction is prevalent to use and it could improve the stability of DNA, however, GO is almost not used in electrochemical detection due to its bad electro conductibility. Thus new combination modes between DNA and graphene should be developed. As well known, Michael addition is a very useful reaction in organic chemistry. However, to the best of our knowledge, the assembly of NH_2-ssDNA on graphene via Michael addition reaction has not been reported up to now. Herein, a probe DNA modified at the 5'-end

with an alkylamino modifier (NH_2-ssDNA) was premeditated to be grafted on the reduced graphene oxide (RGO) surface via Michael addition reaction.

Our solving strategy for grafting NH_2-ssDNA was inspired by the fact that the catecholaminergic neurotransmitter dopamine (DA) will undergo self-polymerization to produce an adherent polydopamine (PDA) in a weak base environment (Lee et al., 2007), which contains catechol and quinone functional groups and reacts with amines via Michael addition reaction (Lee et al., 2007; Tu et al., 2007; Golabi et al., 2003). Meanwhile, due to these fascinating properties of dopamine such as reducibility, self-polymerization and adhesive, it can be utilized as a reducing agent for GO and a capping agent to stabilize and decorate the resulting RGO surface for further functionalization (Xu et al., 2010). Therefore, dopamine was selected as reducer for reducing graphene oxide to prepare PDA functionalized RGO in the present work. Then NH_2-ssDNA could be successfully grafted on the PDA-RGO surface by Michael addition reaction (Figure 1). In the absence of Hg^{2+}, the target DNA with four thymine-thymine (T-T) mismatches could not hybridize with the probe DNA on the glassy carbon electrode (GCE). While in the presence of Hg^{2+}, they could hybridize through T-Hg^{2+}-T coordination chemistry. Then the hybridization of the two oligonucleotides leads to the increase in the peak currents of $[Ru(NH_3)_6]^{3+}$, which could be used for electrochemical sensing of Hg^{2+}. As far as we know, we report for the first time using Michael addition reaction to build a graphene-NH_2-ssDNA biosensor for sensitive and selective detection of Hg^{2+}. The proposed electrochemical biosensor is rapid, convenient and low-cost for effective sensing of Hg^{2+}. The

detection limit of this biosensor was 5.0×10^{-9} M (S/N=3), which reached the World Health Organization (WHO) and Environmental Protection Agency (EPA) limits of Hg^{2+}. Particularly, the proposed method was applied successfully to the determination of Hg^{2+} detection in real environmental samples.

[Figure 1]

2. Experiment

2.1. Chemical Reagents

The 19 mer oligonucleotides were purchased from Invitrogen Trading (Shanghai) Co., Ltd. The probe DNA is modified at the 5'-end with an alkylamino modifier (NH_2-ssDNA: 5'-NH_2-$(CH_2)_6$-GAT-TCC-GTG-CAT-GAC-TCA-G-3'). The target DNA is four-base mismatch to the probe DNA (4-Mis DNA: 5'-C-TGT-GTC-TTG-CTC-GGT-ATC-3'). The control DNA contains the same sequence to the probe DNA (5'-GAT-TCC-GTG-CAT-GAC-TCA-G-3') was used for control experiment, which was not modified by amine. The sequence of complementary DNA is 5'-C-TGA-GTC-ATG-CAC-GGA-ATC-3', which is complementary to the probe DNA. And the sequence of non-complementary DNA is 5'-C-ATG-ACT-CGA-ACT-AAC-GGC-3'. All the DNA fragments were diluted in the Tris-Cl (10 mM, pH=7.4), then stocked at -15℃ to avoid denaturation. Dopamine (DA, 99%) was purchased from Acros Organics (New Jersey, USA). Graphite powder was purchased from Sinopharm Chemical Reagent Co., Ltd. (Beijing, China). All used chemicals were of analytical reagent grade and solutions were prepared with Milli-Q-purified distilled water.

2.2. Synthesis of Polydopamine-capped Reduced Graphene Oxide

Graphene was synthesized according to a published route involving the steps of graphite oxide, exfoliation and chemical reduction. GO was prepared via the modified Hummers method (Hummers et al., 1958). Then the GO was dissolved in deionized water by sonication in an ice bath for 20 min. 100 mL of the supernatant fluid of GO about 0.1 mg/L were added into 50 mg of dopamine hydrochloride and 100 mL of 20 mM Tris-Cl solution (pH=8.5). The reaction mixture was stirred at 60℃ for 24 h. After completing of the reduction reaction, the PDA-capped RGO was centrifuged and washed repeatedly.

2.3. Synthesis of DNA-Grafted RGO

The PDA-capped RGO was dispersed in 10 mM Tris-Cl solution (pH=8.5), in which 5×10^{-7} M probe DNA (NH_2-ssDNA) was added. The reaction mixture was stirred at 50℃ for 40 h. After that, the solution was centrifuged and washed, then dispersed in deionized water. And then the NH_2-ssDNA-grafted RGO was obtained and stored at 4℃ when not in use. The two-step approach of the NH_2-ssDNA modified RGO through Michael addition reaction is illustrated in Figure 1. In addition, 5×10^{-7} M control DNA mixed with RGO as control experiment in the same conditions as those above.

2.4. Apparatus

The UV-vis spectra were measured with a UV-2550 spectrophotometer (Shimadzu, Japan) at room temperature. The FT-IR spectra were recorded in KBr pellets in the frequency range of 400-4000 cm-1 using Avatar 360 FT-IR ESP spectrometer (Nicolet,

America). X-ray diffraction (XRD) data were collected on MSAL-XD2 using Cu Kα (1.5406A˚) radiation with a 2θ range from 5˚ to 80˚ at a step width of 0.01˚. Scanning electron microscopy (SEM) images were recorded on a Hitachi S-4800 scanning electron microscope (Hitachi, Japan) operated at 10 kV. Transmission electron microscopy (TEM) measurements were performed on an Tecnai G2 20 S-TWIN transmission electron microscope at 80 kV. X-ray photoelectron spectroscopy (XPS) data were obtained with an ESCALab220i-XL electron spectrometer from VG Scientific using 300W Al Kα radiation. Tapping mode atomic force microscopy (AFM) images were taken by a Multimode SPM with a Nanoscope Ⅲ Digital Instrument. All of the pH measurements were performed with PB-10 pH meter (Sartorius, Germany).

2.5. Electrochemical Measurements

All electrochemical measurements including differential pulse voltammetry (DPV), cyclic voltammetry (CV), and electrochemical impedance spectroscopy (EIS) were performed at room temperature using a CHI 660D electrochemical workstation (Shanghai, China). The three-electrode system was employed with a glassy carbon electrode (GCE, Φ=3mm, CHI) as a working electrode, a platinum wire as an auxiliary electrode, and a saturated calomel electrode (SCE) as a reference electrode. Differential pulse voltammetry (DPV) was recorded in 10 mM Tris-Cl (pH=7.4) containing 50 μM $[Ru(NH_3)_6]^{3+}$ within the potential range from 0 to -0.6 V under a modulation amplitude of 50 mV and a scan rate of 8 mV/s with a step potential of 4 mV. Cyclic voltammograms (CV) was performed in 10 mM Tris-Cl (pH=7.4)

containing 50 μM $[Ru(NH_3)_6]^{3+}$ solution within the potential range from -0.1 to -0.55 V at a scan rate of 50 mV s^{-1}. EIS experiments were conducted in 0.1 M KCl solution containing 2.5 mM $K_3[Fe(CN)_6]$ and 2.5 mM $K_4[Fe(CN)_6]$ in the frequency range from 0.001Hz to 100kHz with 5 mV as the amplitude.

The glassy carbon electrodes were modified with DNA-grafted RGO. Before modification, the bare GCE was polished to a mirror finish with a piece of diamond paper and 0.05 μm alumina slurry sequentially and then cleaned ultrasonically in ethanol and water for 2 min respectively. Then the GCE was clearly washed with water and dried with N_2. After that 8 μL of RGO dispersion was dropped onto the GCE surface and then dried at room temperature. Lastly the modified electrode was obtained. For comparation, the DNA-RGO and control RGO modified electrodes reacted with complementary and non-complementary DNA solution containing 0.1 μM DNA, 1.0 M $NaNO_3$ in 10 mM Tris-Cl buffer (pH=7.4) for 30 min at 40℃, respectively. Electrochemical measurements were performed by DPV.

To detect Hg^{2+} or other metal ions, the DNA-RGO modified electrode was immersed in a solution containing 0.1 μM 4-mis DNA, 1.0 M $NaNO_3$ and a series of different concentration of Hg^{2+} (0~10 μM) or 10 μM other metal ions in 10 mM Tris-Cl buffer (pH=7.4) for 30 min at 40℃. Electrochemical determination of Hg^{2+} or other metal ions was realized by recording the difference in the value of the DPV peak currents of $[Ru(NH_3)_6]^{3+}$ before and after the 4-mis DNA hybridization with the probe DNA in the presence of Hg^{2+} or other metal ions.

2.6. Analysis of environmental water samples

To evaluate the applications of the method in environmental water samples, actual water sample was obtained from Kunyu River (Beijing). The sample was filtered through 0.45 μm filter and digested with brominating agent. Four milliliter sample was directly spiked with 0, 1, 2, 4, 6 mL Hg^{2+} standard solution ($C_{Hg2+}=5\times10^{-8}$ M) and then regulated volume to 10 mL. Afterward, they were analyzed with the proposed method and flame atomic absorption spectroscopy (FAAS) using a spectrometer AA-6800 (Shimadzu, Japan).

3. Results and Discussion

3.1. Characterization of RGO and DNA-Grafted RGO

The reduction process of GO by dopamine in Tris-Cl was monitored by UV-vis absorption spectroscopy. In Figure S1A, the two absorption peaks at 230 and 300 nm characteristic of GO, originating from π-π^* transition of the C=C band and n-π^* transition of the C=O band, respectively (Chen et al., 2011). After reduction of GO and combination with PDA, the PDA-capped RGO depicts a maximum absorption peak at ~270 nm, indicating the formation of restored electronic conjugation structure within the graphene sheets (Li et al., 2008).

The reduction of the oxygen-containing groups in GO was also confirmed by FTIR spectroscopy (Figure S1B). The FTIR spectra of GO shows carbonyl C=O (1726 cm^{-1}), aromatic C=C (1622 cm^{-1}), carboxyl O=C-O (1384 cm^{-1}), and alkoxy C-O (1055 cm^{-1}) stretching vibrational modes. While the FTIR spectra of RGO shows three peaks at 1582 cm^{-1}, 1400 cm^{-1} and 1046 cm^{-1}, which correspond to the aromatic

C=C stretch, O=C-O and C-O stretch, respectively. It is obvious that the absorption band of carbonyl C=O at 1726 cm^{-1} was disappeared, and the characteristic absorption bands of other oxide groups decreased dramatically, indicating that GO has been reduced to RGO.

At the same time, XRD patterns of the GO and RGO are recorded in Figure S2. The feature diffraction peak of exfoliated GO appears at ~11° (002) is observed with interlay space (d-spacing) of 0.8 nm (Figure S2, a). This value is larger than the d-spacing (0.34 nm) of pristine graphite, as a result of the oxygenated functional groups inserted in carbon sheets. For the resulting RGO (Figure S2, b), the peak located at 11° disappeared, confirming the reduction of GO (Shin et al., 2009).

The surface topography and structure of RGO was measured with scanning electron microscopy (SEM) and transmission electron microscopy (TEM) (Figure S3). The images clearly illustrate the flake-like shapes with sharp edges and ripples. The atomic force microscopy (AFM) image of RGO was shown in Figure 2. The flake-like nanostructures are obviously observed. The average thickness of PDA-capped RGO was about 2 nm, thicker than the average topographic height of single-layer reduced graphite oxide which was approximately 1 nm (Rao et al., 2009). The greater thickness of PDA-capped RGO could be attributed to the PDA coating grafted onto both sides of RGO. In addition, the obvious fluctuation of the height of PDA-capped RGO also indicated that the PDA had been coated on the RGO surface.

[Figure 2]

X-ray photoelectron spectroscopy (XPS) is a significant measurement to observe

the surface functional groups of carbon-based materials. Figure 3A shows that the C1s spectrum of PDA-capped RGO can be curve-fitted into five peak components with binding energy at about 284.6, 285.6, 286.5, 287.9 and 288.8 eV, corresponding to the C-C, C-N, C-O, C=O and O-C=O species, respectively (Wagner et al., 1992). The N1s spectrum of RGO (Figure 3B) shows a peak located in the range of 401.0–401.7 eV, resulting from the interaction between the amino nitrogen and the oxygen-containing surface contaminations (Cui et al., 2007). And the peak located in the range of 400.0–400.3 eV, corresponding to pyrrolic-N (Yun et al., 2012; Zhang et al., 2011b) of PDA. Therefore, both C1s and N1s spectrum of RGO further indicate that PDA was capped on the surface of RGO. As shown in Figure 3C, when RGO mixed with the control DNA，the N1s spectrum presented a new peak at 399.65 eV, showing that the adsorption of the control DNA on RGO (Vilar et al., 2008). When RGO was mixed with the NH_2-ssDNA，the new peak in the N1s spectrum was at 399.51 eV, shifted approximately 0.14 eV (Figure 3D). Reports have shown that the bond formation between the molecules and the substrate will lead to lower binding energy (Petrovykh et al., 2003; Lee et al., 2006). Thus we infer that the shift of binding energy might be due to the amine group of NH_2-ssDNA bonded with benzene ring of PDA through Michael addition reaction, i.e. the probe DNA (NH_2-ssDNA) have been successfully grafted on the PDA capped RGO surface.

[Figure 3]

3.2. Cyclic voltammograms

The electrochemical behavior of the modified electrode was characterized by cyclic

voltammetry using $[Ru(NH_3)_6]^{3+}$ as an electroactive probe. Figure 4A shows the cyclic voltammograms (CVs) of $[Ru(NH_3)_6]^{3+}$ obtained at the bare GCE (a), modified GCE by RGO (b), NH_2-ssDNA-RGO(c) and NH_2-ssDNA-RGO hybridized with 4-mis DNA with the help of 10 μM Hg^{2+} (d), respectively. Compared with the bare GCE, the amperometric response of the modified electrodes increased remarkable, confirming that the modifiers had been successfully modified on GCEs surface. It is noticeable that the response from electrode modified with the probe NH_2-ssDNA is stronger than that modified with RGO, since large numbers of $[Ru(NH_3)_6]^{3+}$ molecules with the ability of binding to the anionic phosphate of DNA backbone. In the presence of Hg^{2+}, the probe NH_2-ssDNA will hybridize with 4-mis DNA through T-Hg^{2+}-T structure (Figure 1), thus both the anodic and cathodic peak currents further increased as larger numbers of $[Ru(NH_3)_6]^{3+}$ molecules binding to the anionic phosphate of double strands DNA (Miao et al., 2009), i.e. the presence of Hg^{2+} leads to the difference in the value of the peak currents of $[Ru(NH_3)_6]^{3+}$. Then the difference in the value of the peak currents of $[Ru(NH_3)_6]^{3+}$ before and after DNA hybridization could be used to detect Hg^{2+}. Therefore, highly sensitive detection of Hg^{2+} could be realized by the proposed method.

[Figure 4]

3.3. Impedance analysis

As further proof, electrochemical impedance spectroscopy (EIS) was carried out using $[Fe(CN)_6]^{3-/4-}$ as the electrochemical probe. As shown in Figure 4B, when GO was modified onto the GCE surface, the semicircle associated with electron-transfer

resistance increased obviously, suggesting that GO inhibits the rate of electron transfer due to its bad conductivity (Xue et al., 2011). However, after RGO was modified on the surface of GCE, the semicircle decreased distinctively, indicating that RGO could accelerate the electron transfer between the electrochemical probe $[Fe(CN)_6]^{3-/4-}$ and the GCE although its electron transfer resistance is still much bigger than that of bare GCE. When RGO mixed with the probe NH_2-ssDNA, the semicircle increased, indicating that the probe NH_2-ssDNA has been grafted on RGO. In the presence of Hg^{2+}, the probe NH_2-ssDNA modified electrode reacted with the four-base mismatches target DNA solution, the semicircle further increased, indicating that the probe DNA hybridized with 4-mis DNA through T-Hg^{2+}-T structure.

3.4. Effect of experimental temperature on the Hg^{2+} sensor

The effect of reaction temperature on the response of the sensor was investigated. The probe NH_2-ssDNA modified GCE hybridized with 4-mis DNA with the help of 10 μM Hg^{2+} at 30℃, 40℃ and 50℃, respectively. The difference in the value of the peak currents of $[Ru(NH_3)_6]^{3+}$ before and after hybridization was 2.87 μA, 3.94 μA and 3.78 μA, respectively. It is obvious that the difference in the value of the peak currents of $[Ru(NH_3)_6]^{3+}$ before and after hybridization at 40℃ was bigger than that at 30℃ or 50℃, thus 40℃ was selected as experimental temperature to realize the sensitive determination of Hg^{2+} in our study.

3.5 Control Experiment

To compare the characteristics of DNA-RGO modified GCEs with those of control

RGO modified GCEs, hybridization of them with complementary DNA and non-complementary DNA was conducted, respectively. The differential pulse voltammetry (DPV) responses were shown in Figure S4, showing that the amperometric response of $[Ru(NH_3)_6]^{3+}$ at the DNA-RGO modified GCEs after being immersed into complementary DNA is much stronger than that into non-complementary DNA, indicating that the DNA-RGO hybridized with the complementary DNA (Figure S4A). However, there is no significant difference for the amperometric responses of the control RGO modified GCEs after being immersed into complementary DNA or non-complementary DNA, indicating that the control RGO did not hybridize with the complementary DNA (Figure S4B). Thus the DNA-RGO (NH_2-ssDNA-grafted RGO) was selected for detection of Hg^{2+} with T-T mismatches in the present work.

3.6. Quantitative determination of Hg^{2+} by differential pulse voltammetry

Figure 5A shows the DPVs of 50 μM $[Ru(NH_3)_6]^{3+}$ in the presence of different concentrations of Hg^{2+} (0-10μM, a-m) in 10 mM Tris-Cl (pH=7.4) at the DNA-RGO modified GCEs after hybridization with the 4-mis DNA. The presence of Hg^{2+} induced an obvious increase of peak currents of $[Ru(NH_3)_6]^{3+}$ at the modified GCEs. The increase in the peak currents of $[Ru(NH_3)_6]^{3+}$ is attributed to the strong interaction between $[Ru(NH_3)_6]^{3+}$ and the double strand DNA, which is produced by the hybridization of the 4-mis DNA with the probe DNA through T-Hg^{2+}-T coordination chemistry. Thus the difference in the value of the peak currents of $[Ru(NH_3)_6]^{3+}$ before and after hybridization could be used for electrochemical sensing

of Hg^{2+}. Figure 5B shows that the difference in the value of the peak currents (ΔI) of 50μM $[Ru(NH_3)_6]^{3+}$ was linearly dependent on the concentrations of Hg^{2+} in the range from 8.0×10^{-9} to 1.0×10^{-7} M, with a coefficiency of 0.996. The detection limit is 5.0×10^{-9} M, which was calculated by 3 times signal-to-noise ratio.

[Figure 5]

In addition, the results obtained above were compared with those of recently reported methods. The advantages of the proposed method over other methods are as follows: First, graphene oxide (GO) was reduced by dopamine, and then the single-strand probe DNA modified at the 5'-end with an alkylamino modifier (NH2-ssDNA) was grafted on the reduced graphene oxide (RGO) surface via Michael addition reaction, which was stable. Second, the proposed method has a lower detection limit (Table 1).

[Table 1]

3.7. The Selectivity for Hg^{2+} Detection

The influences of some other heavy metal ions including Zn^{2+}, Cu^{2+}, Ag^{+}, Cd^{2+}, Pb^{2+}, Fe^{3+}, Fe^{2+}, Co^{2+}, Mn^{2+}, Mg^{2+}, Ca^{2+}, and Ni^{2+} on the determination of Hg^{2+} were investigated. Figure S5 shows that these heavy metal ions even at a high concentration have little effect on the detection of Hg^{2+}, which is in accordance with the previous report (Tanaka et al., 2007). This reveals that the proposed electrochemical biosensor has good selectivity for Hg^{2+} determination.

3.8. Stability and reproducibility of the Hg^{2+} sensor

The NH_2-ssDNA-grafted RGO could be stabilized for several months stored at 4℃. The reproducibility of the proposed Hg^{2+} sensor was examined with DPV measurement. The DPVs of 50 μM $[Ru(NH_3)_6]^{3+}$ in 10 mM Tris-Cl (pH=7.4) were recorded at the DNA-RGO modified GCEs after hybridization with the 4-mis DNA in the presence of 0.1 μM Hg^{2+}. The relative standard deviation was 1.02% for four independent determinations at the same one modified GCE, showing that the proposed Hg^{2+} sensor has good reproducibility.

3.9. Analysis of Environmental Water Samples

To demonstrate its applicability, the proposed method was used in the analysis of Hg^{2+} in river water. The sample was directly spiked with certain amounts of Hg^{2+} standard solution. Hg^{2+} was measured by standard addition method in the real sample. The recovery rates were in good agreement with the results obtained by FAAS, demonstrating the accuracy of the proposed method (Table S1).

4. Conclusion

In conclusion, a novel electrochemical biosensor for sensitive and selective detection of Hg^{2+} based on a DNA grafted graphene is proposed. The hybridization of the two oligonucleotides through T-Hg^{2+}-T coordination chemistry leads to the increase in the peak currents of $[Ru(NH_3)_6]^{3+}$. The difference in the value of the peak currents of $[Ru(NH_3)_6]^{3+}$ before and after DNA hybridization was linear with the concentration of Hg^{2+} in the range from 8.0×10^{-9} to 1.0×10^{-7} M with a linear

coefficiency of 0.996. The detection limit was 5.0×10^{-9} M. The proposed method is rapid, convenient and low-cost for effective sensing of Hg^{2+}. Particularly, the proposed method was applied successfully to the determination of Hg^{2+} detection in real environmental samples.

Acknowledgments

This work was supported by a grant from the Major National Scientific Research Plan of China (973 Program) (Grant No. 2011CB933202), the National Natural Science Foundation of China (Grant Nos. 21205132 and 20972183) , Key Projects in the National Science & Technology Pillar Program during the Eleventh Five-Year Plan Period (Grant No. 2009BAK61B01), National Sci-Tech Major Special Item for Water Pollution Control and Management (Grant No. 2009ZX07527-007-003) and the State Key Laboratory of Environmental Chemistry and Ecotoxicology (Grant No. KF2010-23).

References

Aragay, G., Pons, J., Merkoçi, A., 2011. Chem. Rev. 111, 3433–3458.

Bernaus, A., Gaona, X., Esbrí, J. M., Higueras, P., Falkenberg, G., Valiente, M., 2006. Environ. Sci. Technol. 40, 4090–4095.

Bonanni, A., Pumera, M., 2011. ACS Nano 5, 2356–2361.

Bonanni, A., Ambrosi, A., Pumera, M., 2012. Chem. Eur. J. 18, 1668–1673.

Butler, O. T., Cook, J. M., Harrington, C. F., Hill, S. J., Rieuwerts, J., Miles, D. L., 2007. J. Anal. Atom. Spectrom. 22, 187–221.

Chen, J. L., Yan, X. P., Meng, K., Wang, S. F., 2011. Anal. Chem. 83, 8787–8793.

Chen, K., Lu, G. H., Chang, J. B., Mao, S., Yu, K. H., Cui S. M., Chen J. H., 2012. Anal. Chem. 84, 4057−4062.

Cui, N. Y., Liu, C. Z., Brown, N. M. D., Meenan, B. J., 2007. Appl. Surf. Sci. 253, 6932–6938.

Dave, N., Chan, M. Y., Huang, P. J., Smith, B. D., Liu, J. W., 2010. J. Am. Chem. Soc. 132, 12668–12673.

Dubuisson, E., Yang, Z. Y., Loh, K. P., 2011. Anal. Chem. 83, 2452–2460.

Fang, Z., Pu, K. E., Liu, B. 2008. Macromolecules 41, 8380–8387.

Feng, L. Y., Chen, Y., Ren, J. S., Qu X. J., 2011. Biomaterials 32, 2930–2937.

Geim, A. K., Novoselov, K. S., 2007. Nature Mater. 6, 183–191.

Golabi, S.M., Nourmohammadi, F., Saadnia, A., 2003. J. Electroanal. Chem. 548, 41–47.

Gu, Z., Zhao, M. X., Sheng, Y. W., Bentolila, L, A., Tang, Y., 2011. Anal. Chem. 83,

2324–2329.

Harris, H. H., Pickering, I. J., George, G. N., 2003. Science 301, 1203.

Helwa, Y., Dave, N., Froidevaux, R., Samadi, A., Liu, J. W., 2012. ACS Appl. Mater. Interfaces 4, 2228–2233.

Hummers, W. S., Offeman, R. E., 1958. J. Am. Chem. Soc. 80, 1339–1339.

Hung, Y. L., Hsiung, T. M., Chen, Y. Y., Huang, Y. F., Huang, C. C., 2010. J. Phys. Chem. C 114, 16329–16334.

Joseph, K. A., Dave, N., Liu, J. W., ACS Appl. 2011. Mater. Interfaces 3, 733–739. [4] Wu, D. Y., Huang, W., Duan, C. Y., Lin, Z. H., Meng, Q. J., 2007. Inorg. Chem. 46, 1538–1540.

Kim, T. H., Lee, J., Hong, S., 2009. J. Phys. Chem. C 113. 19393–19396.

Lee, M. H., Lee, S. W., Kim, S. H., Kang, C. H., Kim, J. S., 2009. Org. Lett. 11, 2101–2104.

Lee, J. S., Mirkin, C. A., 2008. Anal. Chem. 80, 6805–6808.

Lee, H., Dellatore, S. M., Miller, W. M., Messersmith, P. B., 2007. Science 318, 426–430.

Lee, C. Y.; Gong, P., Harbers, G. M., Grainger, D. W., Castner, D. G., Gamble, L. J., 2006. Anal. Chem. 78, 3316–3325.

Li, D., Muller, M. B., Gilje, S., Kaner, R. B., Wallace, G. G., 2008. Nat. Nanotechnol. 3, 101–105.

Liu, Q., Peng, J. J., Sun, L. N., Li, F. Y., 2011. ACS Nano 5, 8040–8048.

Liu, D. B., Qu, W. S., Chen, W. W., Zhang, W., Wang, Z., Jiang, X. Y., 2010. Anal.

Chem. 82, 9606–9610.

Lu, C. H., Yang, H. H., Zhu, C. L., Chen, X., Chen, G. N., 2009. Angew. Chem. Int. Ed. 48, 4785–4787.

McNicholas, T. P., Zhao, K., Yang, C. H., Hernandez, S. C., Mulchandani, A., Myung, N. V., Deshusses, M. A., 2011. J. Phys. Chem. C 115, 13927–13931.

Meyer, J. C., Geim, A. K., Katsnelson, M. I., Novoselov, K. S., Booth, T. J., Roth, S., 2007. Nature 446, 60–63.

Miao, P., Liu, L., Li, Y., Li, G., 2009. Electrochem. Commun. 11, 1904–1907.

Miyake, Y., Togashi, H., Tashiro, M., Yamaguchi, H., Oda, S., Kudo, M., Tanaka, Y., Kondo, Y., Sawa, R., Fujimoto, T., Machinami, T., Ono, A., 2006. J. Am. Chem. Soc. 128, 2172–2173.

Mo, Z. H., Yang, L. L., Yang X. C., Chen, Z. F., 2009. Chinese J. Anal. Chem. 37, 1033–1036.

Novoselov, K. S., Geim, A. K., Morozov, S. V., Jiang, D., Katsnelson, M. I., Grigorieva, I. V., Dubonos, S. V., Firsov, A. A., 2005. Nature 438, 197–200.

Petrovykh, D. Y., Kimura-Suda, H., Whitman, L. J., Tarlov, M., 2003. J. Am. Chem. Soc. 125, 5219–5226.

Pumera, M., 2010. Chem. Soc. Rev. 39, 4146–4157.

Rao, C. N. R., Sood, A. K., Subrahmanyam, K. S., Govindaraj, A., 2009. Angew. Chem. Int. Ed. 48, 7752-7777.

Shin, H. J., Kim, K. K., Benayad, A., Yoon, S. M., Park, H. K., Jung, I. S., Jin, M. H., Jeong, H. K., Kim, J. M., Choi, J. Y., 2009. Adv. Funct. Mater. 19, 1987–1992.

Stine, R., Robinson, J. T., Sheehan, P. E., Tamanaha, C. R., 2010. Adv. Mater. 22, 5297–5300.

Stobiecka, M., Molinero, A. A., Chalupa, A., Hepel, M., 2012. Anal. Chem. 84, 4970–4978.

Tanaka, Y., Oda, S., Yamaguchi, H., Kondo, Y., Kojima, C., Ono, A., 2007. J. Am. Chem. Soc. 129, 244–245.

Tang, L. A. L., Wang, J. Z., Loh, K. P., 2010a. J. Am. Chem. Soc. 132, 10976–10977.

Tang, Z. W., Wu, H., Cort, J. R., Buchko, G. W., Zhang, Y. Y., Shao, Y. Y., Aksay, I. A., Liu, J., Lin, Y. H., 2010b. Small 6, 1205–1209.

Tang, L. H., Wang, Y., Liu, Y., Li, J. H., 2011. ACS Nano 5, 3817–3822.

Tu, X. M., Xie, Q. J., Huang, Z., Yang, Q., Yao, S. Z., 2007. Electroanalysis 17, 1815–1821.

Vilar, M. R., Botelho do Rego, A. M., Ferraria, A. M., Jugnet, Y., Nogue`s, C., Peled, D., Naaman, R., 2008. J. Phys. Chem. B 112, 6957–6964.

Wagner, C. D., Moulder, J. F., Davis, J. E., Riggs, W. M., 1992. In Handbook of X-ray Photoelectron Spectroscopy; Perkin-Elmer Corp.: Waltham, MA, pp 40, 45, 73.

Wang, K., Ruan, J., Song, H., Zhang, J. L., Wo, Y., Guo, S. W., Cui, D. X., 2011. Nanoscale Res. Lett. 6, 8.

Wen, S., Zeng, T., Liu, L., Zhao, K., Zhao, Y. J., Liu, X. J., Wu, H. C., 2011. J. Am. Chem. Soc. 133, 18312–18317.

Wu, D. H, Zhang, Q., Chu, X., Wang, H. B., Shen, G. L., Yu, R. Q., 2010, Biosens. Bioelectron. 25, 1025–1031.

Wu, M., Kempaiah, R., Huang, P. J., Maheshwari, V., Liu, J. W., 2011. Langmuir 27, 2731-2738.

Xu, L. Q., Yang, W. J., Neoh, K. G., Kang, E. T., Fu, G. D., 2010. Macromolecules 43, 8336–8339.

Xue, Y., Zhao, H., Wu, Z. J., Li, X. J., He, Y. J., Yuan, Z. B., 2011. Biosens. Bioelectron. 29, 102–108.

Yun, J. M., Kim, K. N., Kim, J. Y., Shin, D. O., Lee, W. J., Lee, S. H., Lieberman, M., Kim, S. O., 2012. Angew. Chem. Int. Ed. 51, 912–915.

Zhang, Y. B., Tan, Y. W., Stormer, H. L., Kim, P., 2005. Nature 438, 201–204.

Zhang, M., Yina, B. C., Tan, W. H., Yea, B. C., 2011a. Biosens. Bioelectron. 26, 3260–3265.

Zhang, C. H., Fu, L., Liu, N., Liu, M. H., Wang, Y. Y., Liu, Z. F., 2011b. Adv. Mater. 23, 1020–1024.

Zhang, Y. F., Yuan, Q., Chen, T., Zhang, X. B., Chen, Y., Tan, W. H., 2012. Anal. Chem. 84, 1956−1962.

Zhao, Y., Zhong, Z., 2006. J. Am. Chem. Soc. 128, 9988–9989.

Zhao,X., Zhang, Q. H., Chen, D. J., Lu, P., 2010. Macromolecules 43, 2357–2363.

Captions for Figures

Figure 1. Illustration of the procedure for preparing PDA-capped RGO and the graft of NH_2-ssDNA on RGO surface through a covalent binding strategy and the mechanism of detection of Hg^{2+}.

Figure 2. Tapping mode AFM images of RGO and height profiles along the lines shown in AFM images of RGO.

Figure 3. X-ray photoelectron spectroscopy (XPS) C1s spectra of RGO (A) and N1s spectra of RGO (B), control DNA-RGO (C) and NH_2-ssDNA-RGO (D).

Figure 4. (A) Cyclic voltammograms of bare GCE (a), RGO modified GCE (b), NH_2-ssDNA-RGO modified GCE (c) and NH_2-ssDNA-RGO modified GCE after hybridizing with 4-mis DNA in the presence of 10 μM Hg^{2+} (d) in 50μM $[Ru(NH_3)_6]^{3+}$ solution at a scan rate of 50 mV s^{-1}. (B) Nyquist plots of bare GCE (a), RGO modified GCE (b), DNA-RGO modified GCE (c), DNA-RGO modified GCE after hybridized with 10 μM Hg^{2+} (d), and GO modified GCE (e). EIS experiments were conducted in 0.1M KCl solution containing 2.5 mM $K_3[Fe(CN)_6]$ and 2.5 mM $K_4[Fe(CN)_6]$. The insets show the whole EIS plot of bare GCE and GO modified GCE.

Figure 5. (A) DPV response curves of the NH_2-ssDNA-RGO modified GCE in 10 mM Tris-Cl (pH=7.4) containing 50 μM $[Ru(NH_3)_6]^{3+}$ solution after hybridization with 4-mis DNA in the presence of different concentrations of Hg^{2+}, from 0 to 10 μM (a-m). (B) The plot of the difference in the value of the peak currents of $[Ru(NH_3)_6]^{3+}$ against the Hg^{2+} concentrations. Error

bars show the standard deviations of measurements taken from three independent experiments. The parameters of DPVs: Amplitude, 50 mV; Pulse width, 0.2 s; pulse period, 0.5 s.

Caption for Table:

Table 1. Performance comparison of the proposal methods for Hg^{2+}.

Graphene oxide (GO) was reduced by dopamine, and then the single-strand probe DNA modified at the 5'-end with an alkylamino modifier (NH_2-ssDNA) was grafted on the reduced graphene oxide (RGO) surface via Michael addition reaction. Thus a novel electrochemical biosensor for sensitive and selective detection of mercury (II) ions (Hg^{2+}) based on T-Hg^{2+}-T coordination chemistry is realized. >A detection limit of 5.0×10^{-9} M Hg^{2+} was obtained (S/N=3). >The proposed method was used to analyze Hg^{2+} in river.

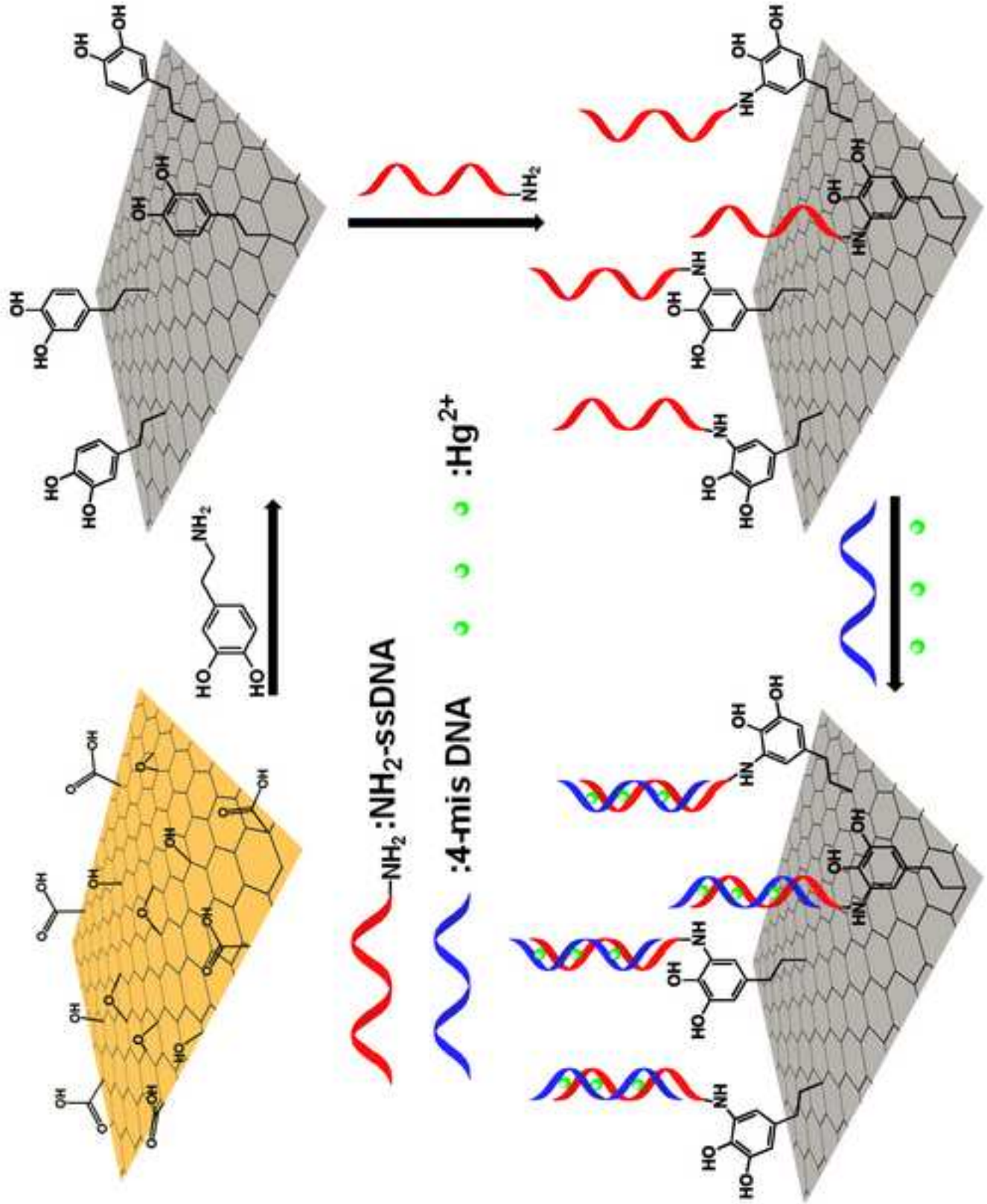

Figure 1

Figure 2

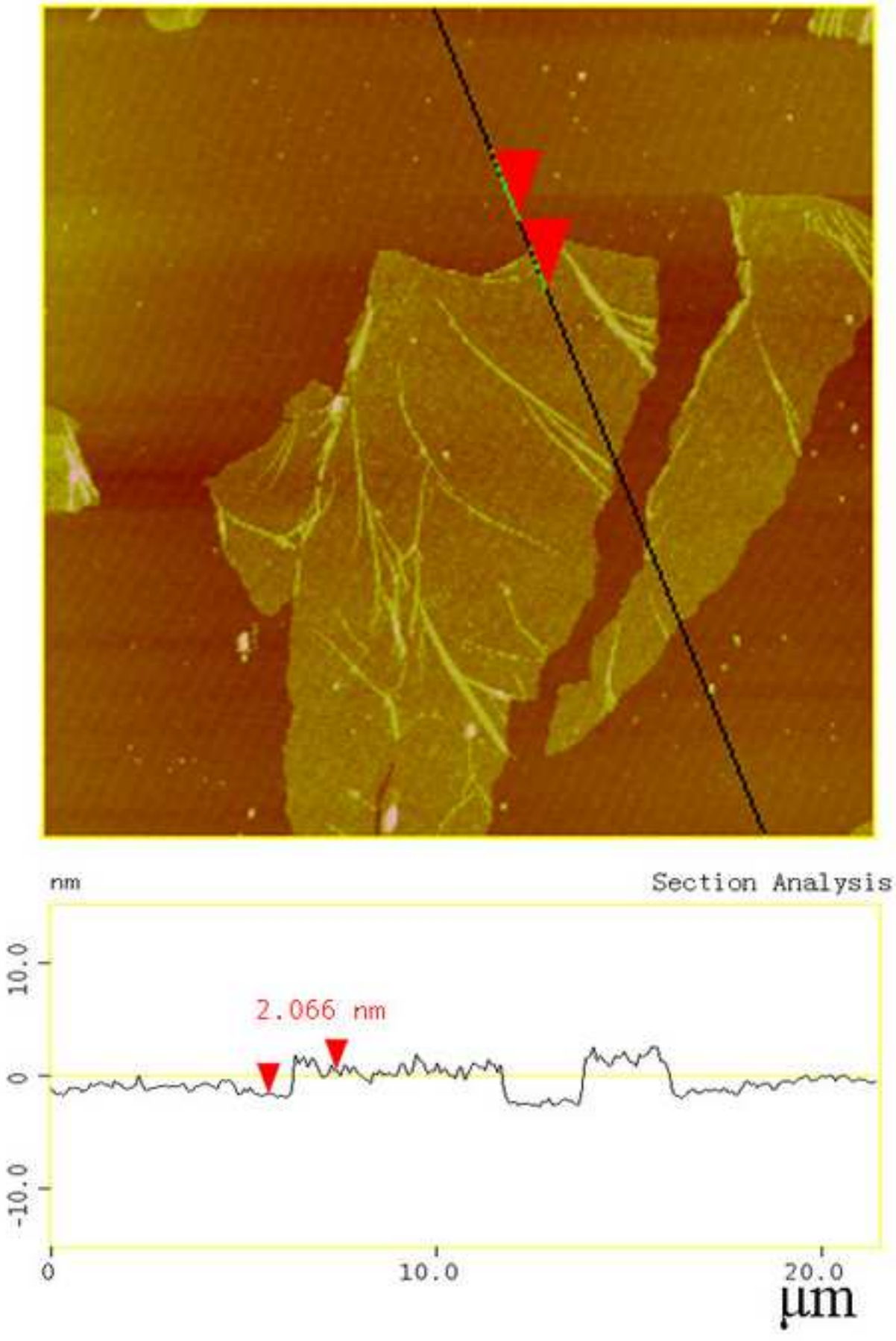

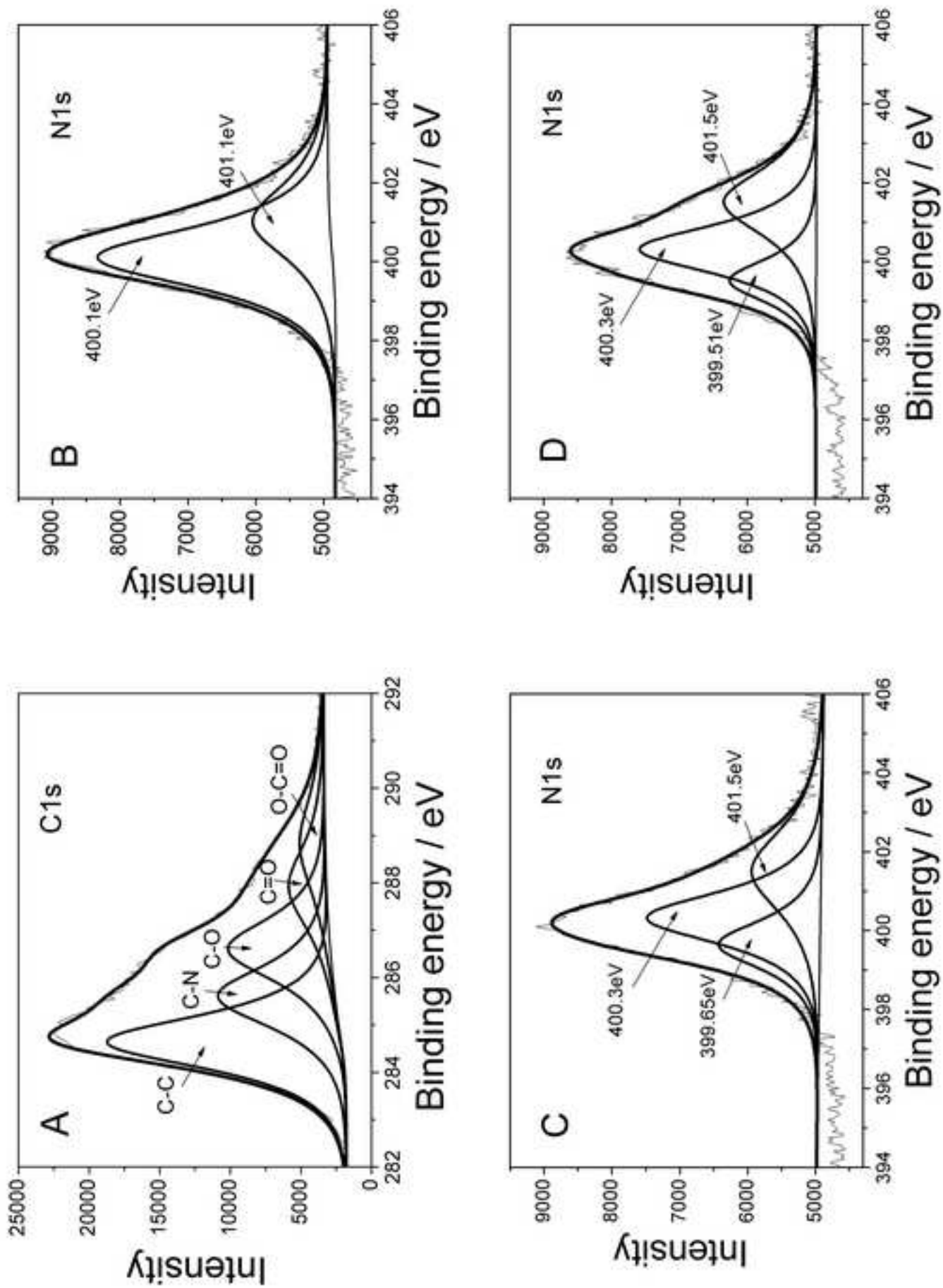
A
C1s
C-C
C-N
C-O
C=O
O-C=O
Intensity
Binding energy / eV
B
N1s
400.1eV
401.1eV
C
N1s
400.3eV
399.65eV
401.5eV
D
N1s
400.3eV
399.51eV
401.5eV

Figure 3

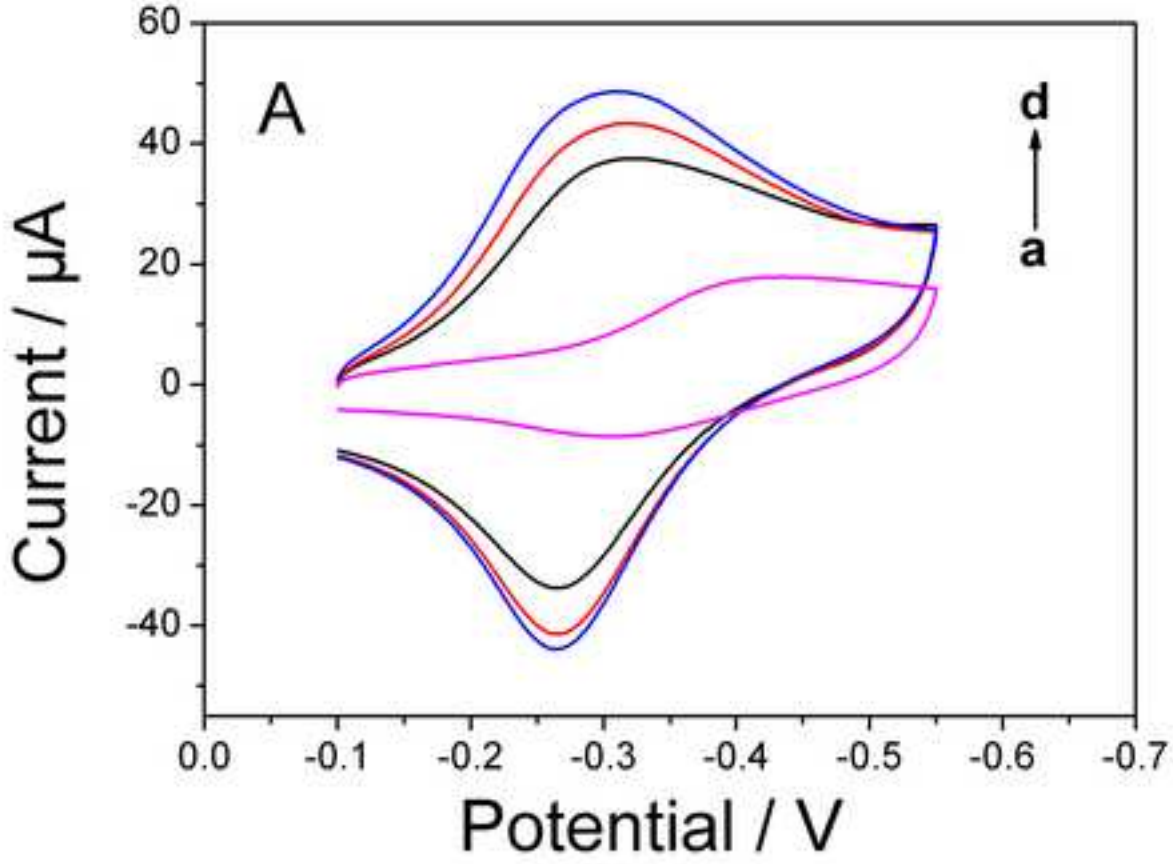

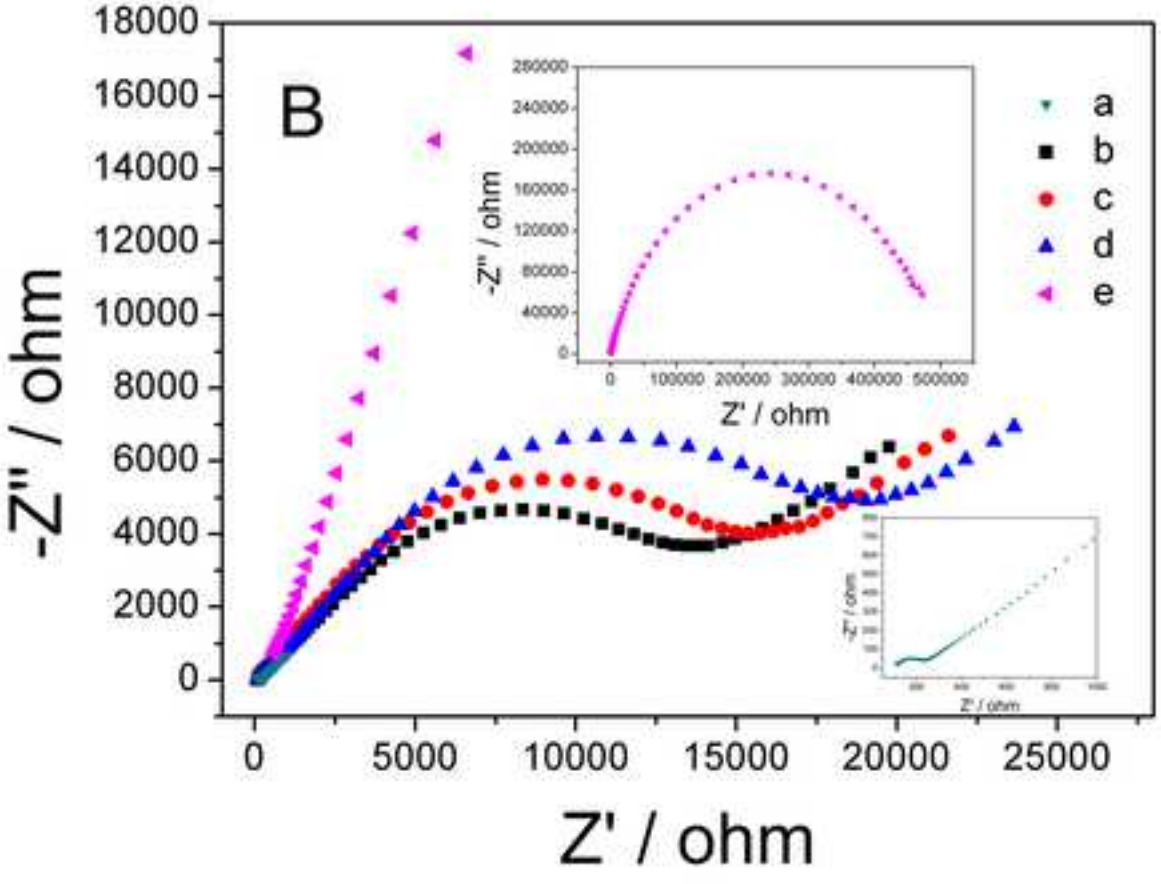

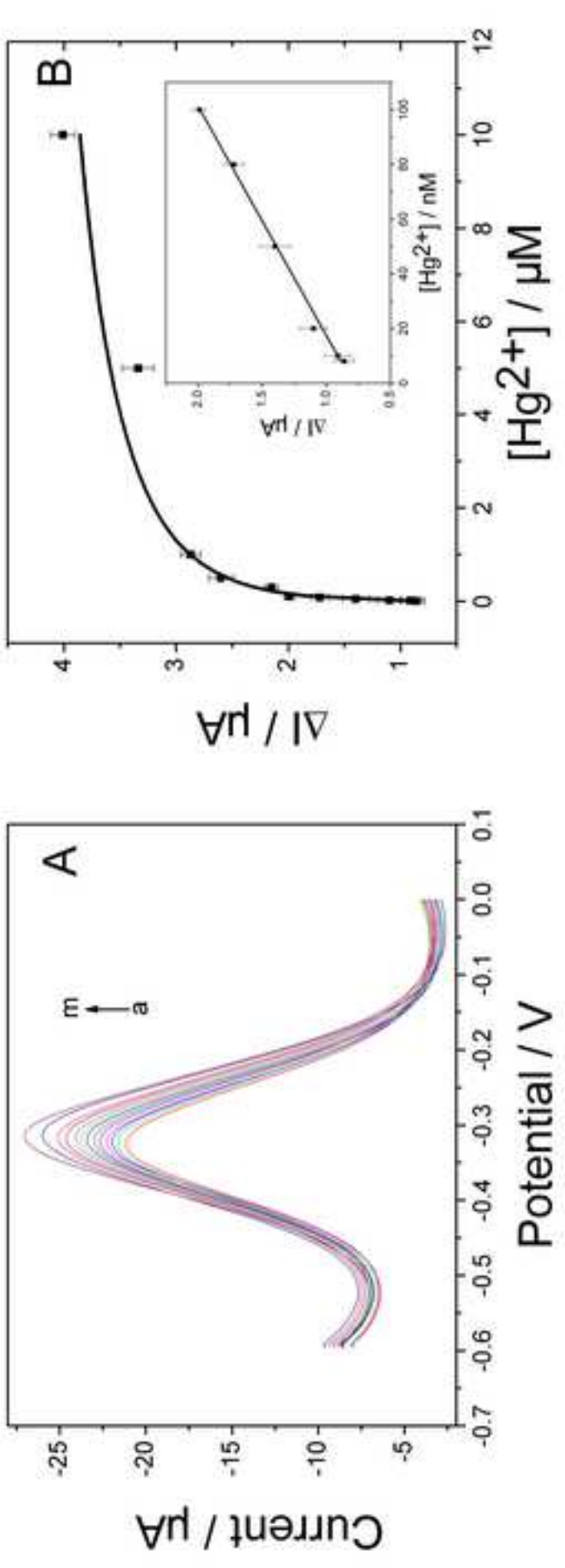

Figure 5

Methods	Linear range	Detection limit	Reference
DNA functionalized Graphene	8 to 100nM	5 nM	This work
Thermally Reduced Graphene Oxide Decorated with Functionalized Gold Nanoparticles		25 nM	Chen et al.,2012
Quaternary Ammonium Group-Capped Gold Nanoparticles	0 to 600 nM	30 nM	Liu et al., 2010
DNA-functionalized silica nanoparticles	0 to 500 nM	20 nM	Zhang et al.2012
Aptamer-Functionalized Hydrogel Microparticles	10 to 200nM	10 nM	Helwa et al., 2012
molecular beacon		19 nM	Stobiecka et al., 2012
Anomalous Response of Carbon Nanotube Conductance		10 nM	Kim et al., 2009